Supporting Information

Dray et al. 10.1073/pnas.1016454108

SI Text

Cytological Analyses of Protein Foci. As expected, DMC1 and RAD51 foci were nearly exclusively associated with chromosome axes (colocalizing with SYCP3) and appeared throughout the nucleus in leptonema and zygotene, but were restricted to the unpaired X chromosome in early pachynema and completely disappeared by late pachynema (Fig. S7 *A–D*). RAD51AP1 staining patterns were qualitatively different, but with some features in common with DMC1 staining. We observed five classes of RAD51AP1 nuclear staining patterns that appeared in a stage-specific manner. Class I foci are axis-associated, and class II foci are nuclear but not axis-associated (colocalizing only with DAPI) (Fig. S7*A*, *Inset*). Both classes were present throughout prophase I (Fig. S7 *A–D*). Class III staining represents the substantial coating of synapsed regions that begins to appear in zygotene (Fig. S7*B*, *Inset*) and culminates in pachytene (Fig. S7*C*, *Inset*), when all autosomal bivalents are fully synapsed. In particular, much of the class III RAD51AP1 staining was coincident with the persistent DMC1 and RAD51 foci that are associated with the unsynapsed portion of the X (and to a lesser extent the Y) during pachytene. However, because class III staining was also observed in the nonhomologously synapsed regions at the zygotene-like stage in chromosome spreads from *Spo11-/-* males where no meiotic double-strand breaks (DSBs) are formed (Fig. S7*F*, *Inset*), we can infer this immunostaining pattern as being HR-independent and therefore unlikely to be informative about interactions of RAD51AP1 with DMC1. Class IV foci are large speckles that appeared both inside and outside of nuclei; when in the nucleus, they were rarely axis-associated (Fig. S7*C*, *Inset*). Because these foci occurred in all meiotic stages and were not diminished by treatment of the anti-RAD51AP1 antibodies with purified RAD51AP1 protein, we interpret them as nonspecific background signal. Finally, class V represents a small number of bright axis-associated foci (typically 1–2) that were observed on most late pachytene bivalents (Fig. S7*D*, *Inset*). This is consistent with a role of RAD51AP1 at later stages of meiosis, but likely independent of its interactions with DMC1 and RAD51.

Analysis of RAD51AP1-RAD51 Colocalization. The cytological analysis to examine the colocalization of RAD51 with RAD51AP1 was conducted as described in the main text for DMC1-RAD51AP1 colocalization test, using 1:200 rabbit anti-RAD51 antibodies (Calbiochem, PC130). We performed rotation tests to verify the significance of the RAD51-RAD51AP1 colocalization results (Fig. S6 *E* and *F*). We first rotated the RAD51 image and observed that the number of axis-associated foci decreased from 64 ± 17 in the true images to 14 ± 5 in the rotated images (Fig. S6*I*, $P = 0.0004$). The spreads with the rotated RAD51AP1 channel displayed an average of 65 ± 16 axis-associated RAD51AP1 foci, as compared to the 84 ± 18 observed in the unrotated nuclei (Fig. S6*I*, $P = 0.0131$). Importantly, before and after rotation of the RAD51AP1 image, the number of RAD51 foci colocalizing with RAD51AP1 decreased from 30 ± 9 to 7 ± 2 ($P = 0.0004$).

SI Materials and Methods.

Purification of RAD51AP1 Mutants. The L319Q and H329A mutant variants of maltose binding protein (MBP)-tagged RAD51AP1 isoform 2 were expressed in *Escherichia coli* and purified as described for the wild-type counterpart (Fig. 1*B*). Human RAD51 was purified as described previously (1).

Affinity Pull-Down Experiments. The affinity pull-down assay involving tagged RAD51AP1 isoforms and RAD51 was performed as described (2). Briefly, 4 μg of each protein was incubated in 30 μL of buffer A (50 mM Tris at pH 7.5, 1 mM DTT, 0.01% Igepal CA-630, 60 mM KCl) for 30 min at 4 °C before the reaction was mixed for 30 min at 4 °C with 8 μL of Amylose-Sepharose resin (New England Biolabs) to immobilize RAD51AP1 via the MPB tag. After washing the beads twice with 200 μL of the same buffer, bound proteins were eluted with 30 μL of 2% SDS. The supernatant (S), wash (W), and SDS eluate (E), 8 μL each, were analyzed by 12% SDS-PAGE and Coomassie blue staining.

Determination of Antibody Specificity. In order to determine the specificity of the antibodies used in the cytological analyses, we incubated the anti-RAD51, anti-DMC1, and anti-RAD51AP1 antibodies (2.5 μg) with their cognate protein antigen (12.5 μg RAD51AP1 or 6.4 μg of either RAD51 or DMC1) for 30 min in 100 μL before use. In the case of the anti-RAD51 and anti-DMC1 antibodies, the treatment specifically abolished the ability of the antibody preparations to reveal foci of their cognate target (Fig. S7 *D* and *E*). In the case of the anti-RAD51AP1 antibodies, we found that all classes of RAD51AP1 foci disappeared subsequent to such treatment except the class IV foci that we consider to be nonspecific (Fig. S7 *A* and *B*). Because the purified proteins used to titrate out the antibodies had not undergone any denaturation treatment, we infer that the antibodies used recognize the native form of their cognate protein antigen. As expected, the preimmune RAD51AP1 serum did not produce any protein foci (Fig. S7*C*).

DNA Substrates. The following oligonucleotides (Integrated DNA Technologies) were used in the DNA mobility shift assay: P1 and P2 for ssDNA and dsDNA; D1, D2, and D3 to prepare the synthetic D-loop structure (see Table S2). DNA was labeled, annealed, and purified as previously described (1).

DNA Mobility Shift Assay. The sequences of the oligonucleotides (Integrated DNA Technologies) used in substrate construction are listed in Table S2. Labeling of DNA and the DNA mobility shift assay with the ssDNA, dsDNA, and D-loop substrates (30 nM each) was carried out as described in our published study (2).

RT-PCR. Juvenile mice were sacrificed at 5, 15, and 21 d post partum (dpp) to obtain testis-specific RNA with an RNeasy Mini kit (Qiagen). *Spo11-/-* mice at 21 dpp were also sacrificed to obtain testis-specific RNA with the same method. The Super-Script One-Step RT-PCR kit (Invitrogen) was used to synthesize cDNA and to amplify the *RAD51AP1* transcript. Four primers were used to detect overlapping regions of the mouse *RAD51AP1* transcript (RT1 to RT4; see Table S2 and Fig. S6*A*). RT-PCR products were analyzed in a 1% agarose gel run in TAE buffer (40 mM Tris acetate, pH 7.4, 2 mM EDTA) and stained with ethidium bromide. DMC1 and β-actin primers were included as positive controls. Each primer pair set also included a minus (−) reverse transcriptase reaction to ensure that there was no genomic DNA contamination.

Western Blotting. Whole cell lysates were prepared from mouse testes (with tunica albuginea removed) by sonication in lysis buffer (60 mM Tris-HCl, pH 6.8, 2% SDS, 10% glycerol, 50 mM dithiothreitol) and resolved by 10% SDS-PAGE. Proteins were transferred to a nitrocellulose membrane for Western analyses.

For RAD51AP1 detection, the nitrocellulose blot was probed with the polyclonal guinea pig antibody GP49, and then with goat anti-guinea pig IgG-HRP (sc-2438, Santa Cruz) as the secondary antibody. For DMC1 and β-actin detection, goat polyclonal anti-DMC1 antibody (sc-8973, Santa Cruz) or mouse monoclonal anti-β-actin antibody (A5316, Sigma) was used as the primary antibody, and either donkey anti-goat IgG-HRP (sc-2020, Santa Cruz) or goat anti-mouse IgG-HRP (sc-2005, Santa Cruz) was used as the secondary antibody.

Immunofluorescence. The immunolocalization of RAD51AP1 with RAD51 was conducted as described in the main text, except that 1:200 rabbit anti-RAD51 antibody (Calbiochem, PC130) was used to detect RAD51.

1. Sigurdsson S, Trujillo K, Song B, Stratton S, Sung P (2001) Basis for avid homologous DNA strand exchange by human Rad51 and RPA. *J Biol Chem* 276:8798–8806.

2. Wiese C, et al. (2007) Promotion of homologous recombination and genomic stability by RAD51AP1 via RAD51 recombinase enhancement. *Mol Cell* 28:482–490.

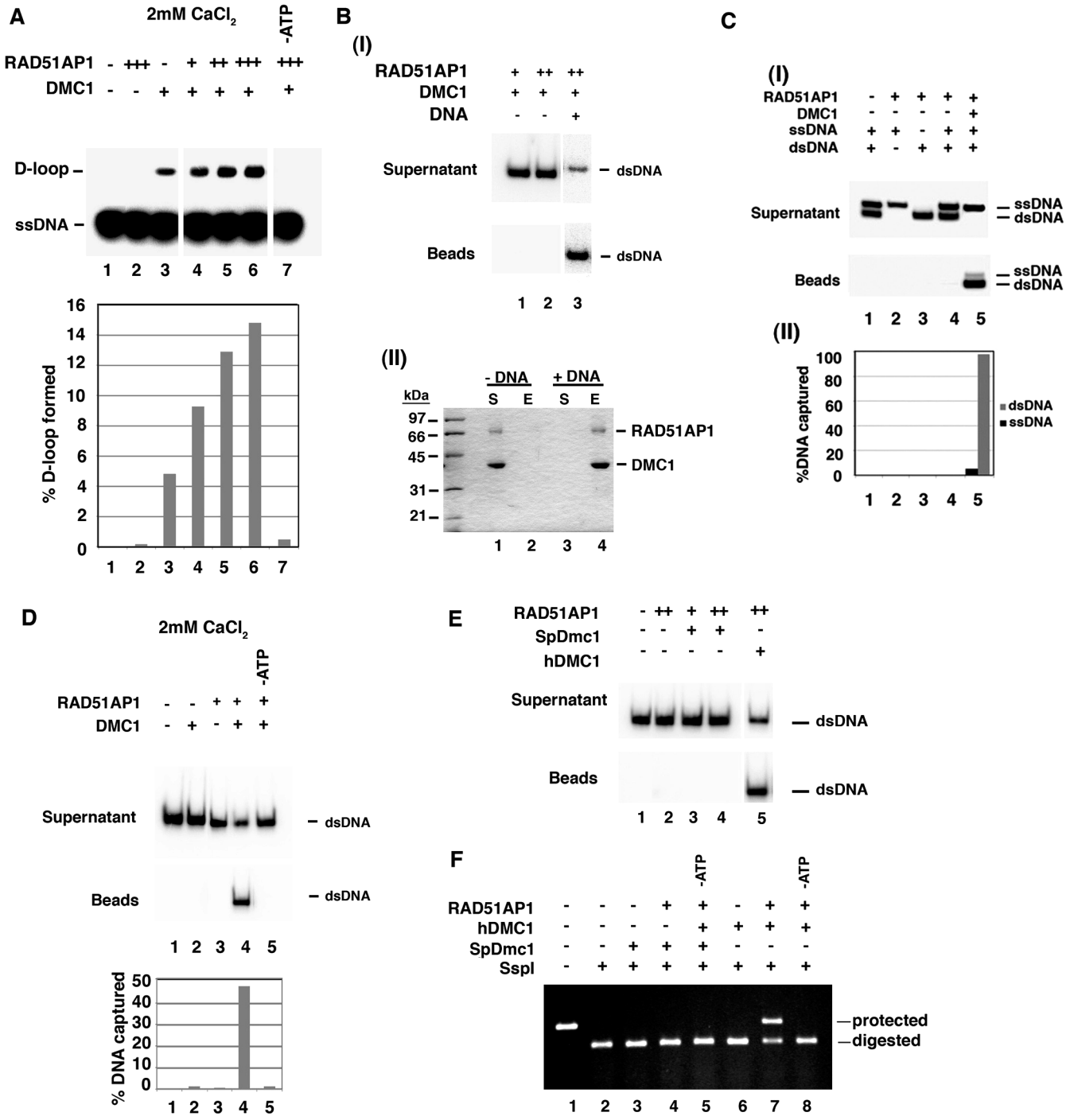

Fig. S1. *GST-tagged RAD51AP1 isoform 2 functionally synergizes with the stabilized DMC1 presynaptic filament but not with the SpDmc1 filament.* (*A*) The D-loop reaction was conducted with RAD51AP1 (200, 300, and 500 nM) and 2 mM $CaCl_2$ to stabilize the DMC1 presynaptic filament. The results were plotted. (*B*) (I) shows that duplex DNA capture did not occur if ssDNA was omitted from the magnetic beads (lanes 1 and 2); a positive control (lane 3) was included. The amount of RAD51AP1 was 300 or 600 nM. (II) shows that DMC1 and RAD51AP1 were retained on the magnetic beads when ssDNA was present (+DNA; lanes 3 and 4) but not when the DNA was omitted (−DNA; lanes 1 and 2). The beads were treated with SDS, and the eluate fraction (designated as *E*) was analyzed along with the supernatant (designated as S). (*C*) When presented with both ssDNA and dsDNA, DMC1 and RAD51AP1 (900 nM) captured the dsDNA preferentially (lane 5). The appropriate controls were included. The results were quantified and plotted (II). (*D*) Duplex capture was examined with RAD51AP1 (300 nM) in the presence of 2 mM $CaCl_2$. The results were plotted. (*E* and *F*) Results showing that RAD51AP1 did not synergize with SpDmc1 in duplex capture (*E*) or synaptic complex assembly (*F*). The amount of RAD51AP1 was 300 or 600 nM in *E* and 500 nM in *F*.

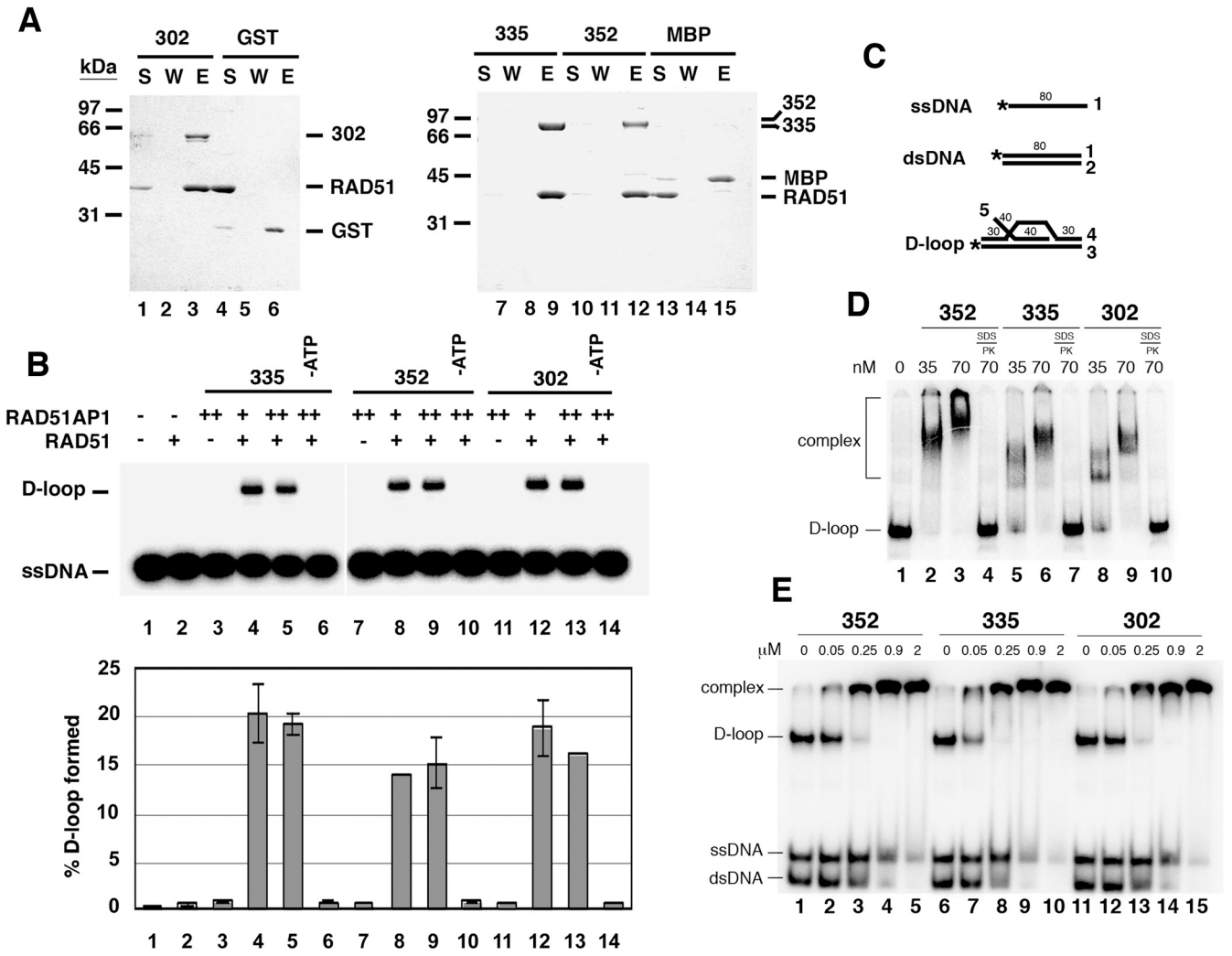

Fig. S2. *Physical and functional interactions of the RAD51AP1 isoforms with RAD51 and DNA*. (*A*) Results from affinity pull-down experiments showing that all three isoforms of RAD51AP1 are capable of RAD51 interaction. (*B*) Results from D-loop reactions showing that all three isoforms of RAD51AP1 are proficient in enhancing the recombinase activity of RAD51. The amount of each RAD51AP1 isoform used was 300 or 500 nM. (*C*) Schematic of the DNA substrates used. The asterisk indicates the oligonucleotide that was radiolabeled. (*D*) DNA mobility shift assay with the indicated concentrations of the three RAD51AP1 isoforms and D loop as a substrate. In lanes 4, 7, and 10, the nucleoprotein complexes were treated with SDS and proteinase K to release the DNA. (*E*) DNA mobility shift assay with the indicated concentrations of the three RAD51 AP1 isoforms and a mixture of D loop, dsDNA, and ssDNA.

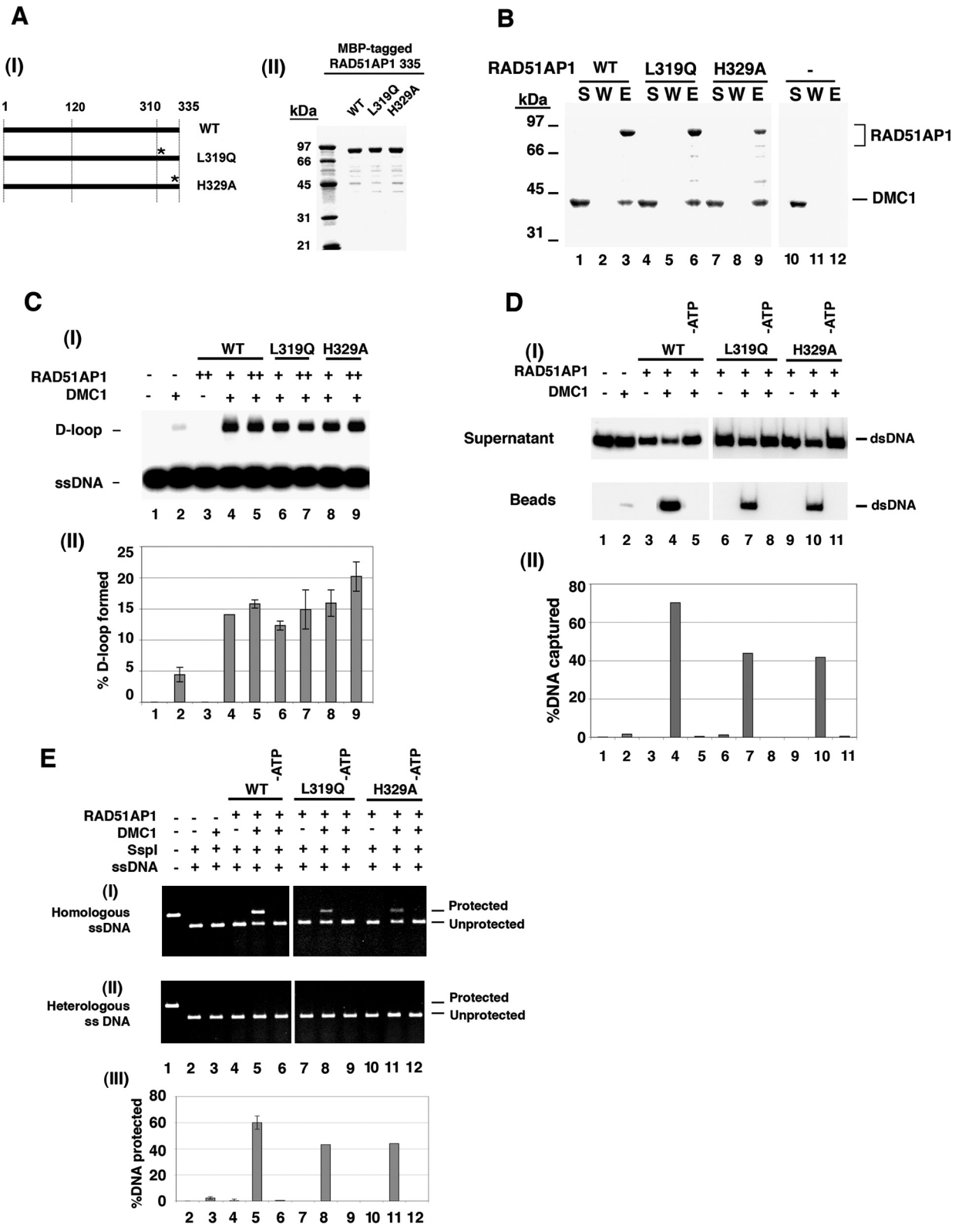

Fig. S3. *Interactions of the MBP-tagged RAD51AP1 L319Q and H329A isoform 2 mutants with DMC1*. (*A*) The RAD51AP1 L319Q and H329A mutant proteins (*i*) were purified and analyzed by SDS-PAGE (*ii*). (*B*) Affinity pull-down assays showing that both the RAD51AP1 L319Q and H329A mutant proteins are capable of complex formation with DMC1. (*C–E*) Results showing that the RAD51AP1 L319Q and H329A mutants are capable of functional synergy with DMC1 in the D-loop reaction (*C*), in duplex capture (*D*), and synaptic complex formation (*E*). The amount of RAD51AP1 or mutants used was 300 or 500 nM in *C* and 500 nM in *D* and *E*.

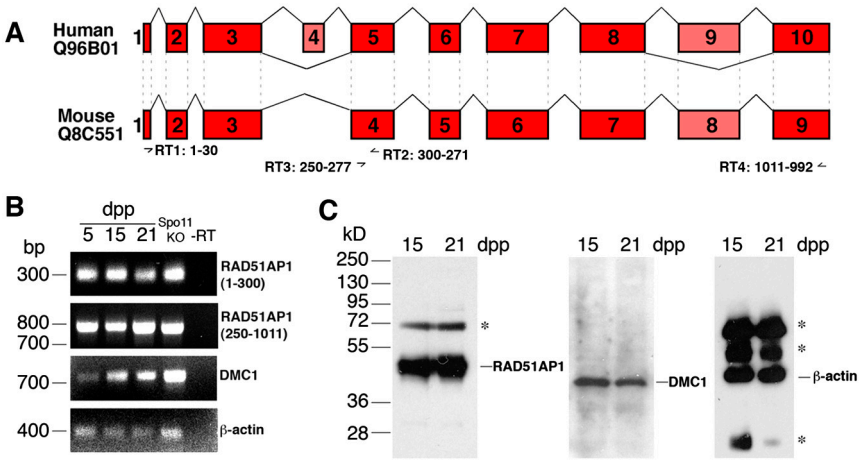

Fig. S4. *Meiotic expression of RAD51AP1*. (*A*) Gene structures of human and mouse *RAD51AP1*, with their Uniprot accession numbers listed below. Human *RAD51AP1* is composed of 10 exons, of which exons 4 and 9 are alternatively spliced to produce three isoforms. Isoform 1 contains all 10 exons, isoform 2 lacks exon 4, and isoform 3 lacks exon 9. Mouse *RAD51AP1* lacks the exon 4 equivalent of the human counterpart but is otherwise organized identically (aligned by the dashed lines). We did not detect the splicing out of exon 8 (equivalent to human exon 9). Location of the RT-PCR primers used for detecting the mouse *RAD51AP1* transcript are indicated by the arrows. (*B*) RT-PCR on total RNA from testes of juvenile wild-type mice of the indicated ages and juvenile *Spo*11$^{-/-}$ mice. PCR without the reverse transcriptase (–RT) was conducted for total RNA from testes of juvenile wild-type mice at 21 dpp as a negative control. DMC1 and β-actin were included as controls in the analysis. (*C*) Western blot analysis of testis extracts from juvenile wild-type mice (15 and 21 dpp) using an antibody (GP49) generated against mouse RAD51AP1 protein, human DMC1, or β-actin. The asterisks denote cross-reacting bands.

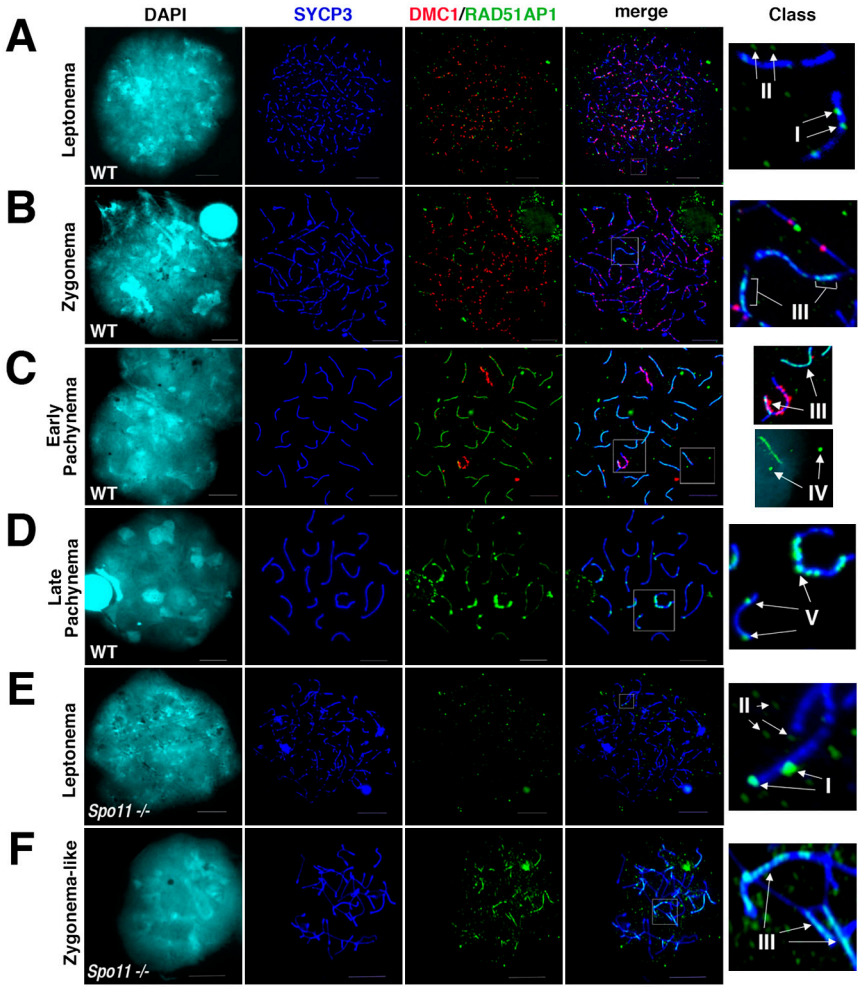

Fig. S5. *RAD51AP1 immunostaining pattern on meiotic chromatin*. Chromosome spreads were stained with anti-SYCP3 (blue), antibody generated against full-length mouse RAD51AP1 protein (green), and anti-DMC1 (red). Scale bar = 10 μm. *A–D* are wild-type spreads; *E* and *F* are *Spo*11$^{-/-}$ spreads. Example of a wild-type spermatocyte nucleus in (*A*) leptonema (a zoomed-in display of the indicated region in the merged image is shown without the DMC1 channel to show class I RAD51AP1 foci that are axis-associated and class II RAD51AP1 foci that are not); (*B*) zygotene (a zoomed-in display of the indicated region in the merged image to show class III RAD51AP1 foci that coat synapsed regions); (*C*) early pachynema (zoomed-in displays of the two indicated regions in the merged image to show class III RAD51AP1 foci that coat synapsed regions and class IV RAD51AP1 foci that are deemed aggregated entities appearing inside and outside the nucleus; the DAPI channel was added to the class IV zoomed-in display); (*D*) late pachynema (a zoomed-in display of the indicated region in the merged image to show class V RAD51AP1 foci that are bright and axis-associated). Example of a *Spo*11$^{-/-}$ spermatocyte nucleus in (*E*) leptonema (a zoomed-in display of the indicated region in the merged image to show class I RAD51AP1 foci that are axis-associated and class II RAD51AP1 foci that are not), and (*F*) zygotene-like (a zoomed-in display of the indicated region in the merged image to show class III RAD51AP1 foci that coat synapsed regions).

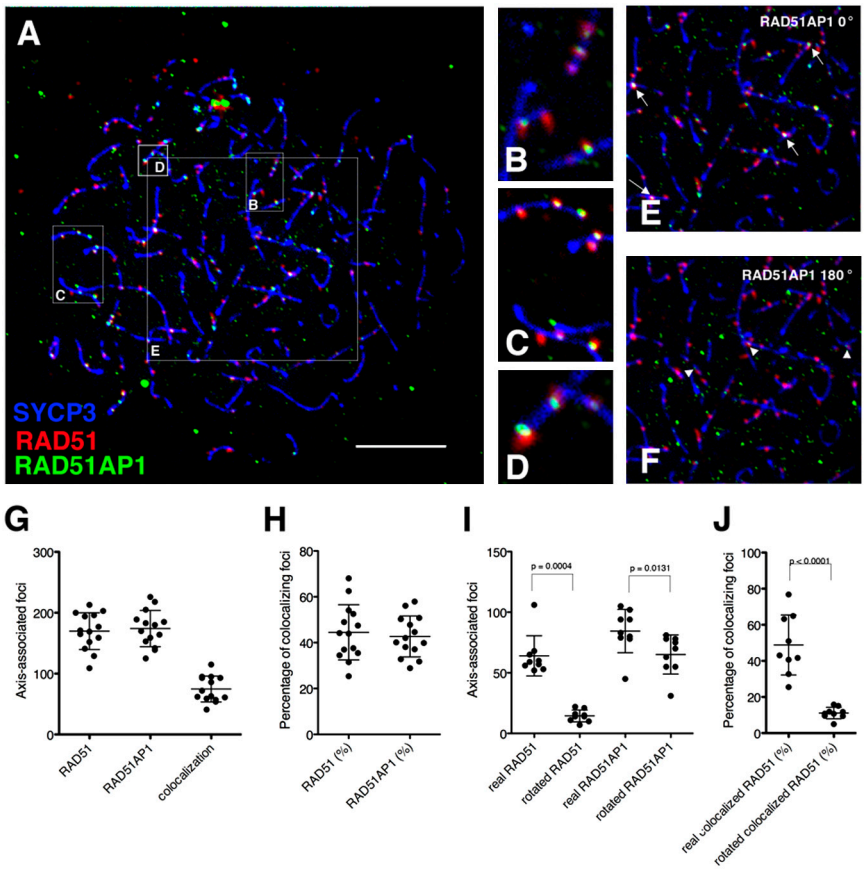

Fig. S6. *Colocalization of RAD51AP1 with RAD51 on meiotic chromatin.* (*A*) Example of a spermatocyte nucleus in leptonema. Chromosome spreads were stained with anti-SYCP3 (blue), anti-RAD51 (red), and anti-RAD51AP1 GP49 (green) antibodies. Scale bar = 10 μm. (*B–D*) Zoomed-in displays of regions indicated in *A* showing colocalized foci of RAD51AP1 and RAD51. Note that foci colocalization was scored without restriction to the subset of foci that share the same centroid. (*E* and *F*) Rotation experiment to evaluate the statistical significance of RAD51AP1-RAD51 colocalization. *E* is a zoomed-in display of the 20 × 20 μm box marked in *A* within which colocalized RAD51AP1 and RAD51 foci were counted, as indicated by white arrows. *F* corresponds to the same region in *E* but with a 180° rotation of the RAD51AP1 immunofluorescence channel. Any RAD51AP1 foci that overlap with RAD51 foci after image rotation, as indicated by white arrowheads, are considered fortuitously colocalized. (*G*) Counts of axis-associated DMC1, RAD51AP1, and colocalized foci in leptotene stage spermatocytes. Each dot represents the count from one nucleus and the same 14 nuclei were quantified (bars = mean ± SD). (*H*) Colocalized foci as a percentage of RAD51 or RAD51AP1 total foci. Each dot represents the percentage from one nucleus and 14 nuclei were quantified (bars = mean ± SD). (*I*) Results of a rotation experiment wherein axis-associated RAD51 or RAD51AP1 foci were counted before and after 180° rotation of the RAD51 or RAD51AP1 immunofluorescence channel. Each dot represents the count from one nucleus and nine nuclei were quantified (bars = mean ± SD). (*J*) Colocalized foci as a percentage of RAD51 total foci before and after 180° rotation of the RAD51AP1 immunofluorescence channel. Each dot represents the count from one nucleus and nine nuclei were quantified (bars = mean ± SD).

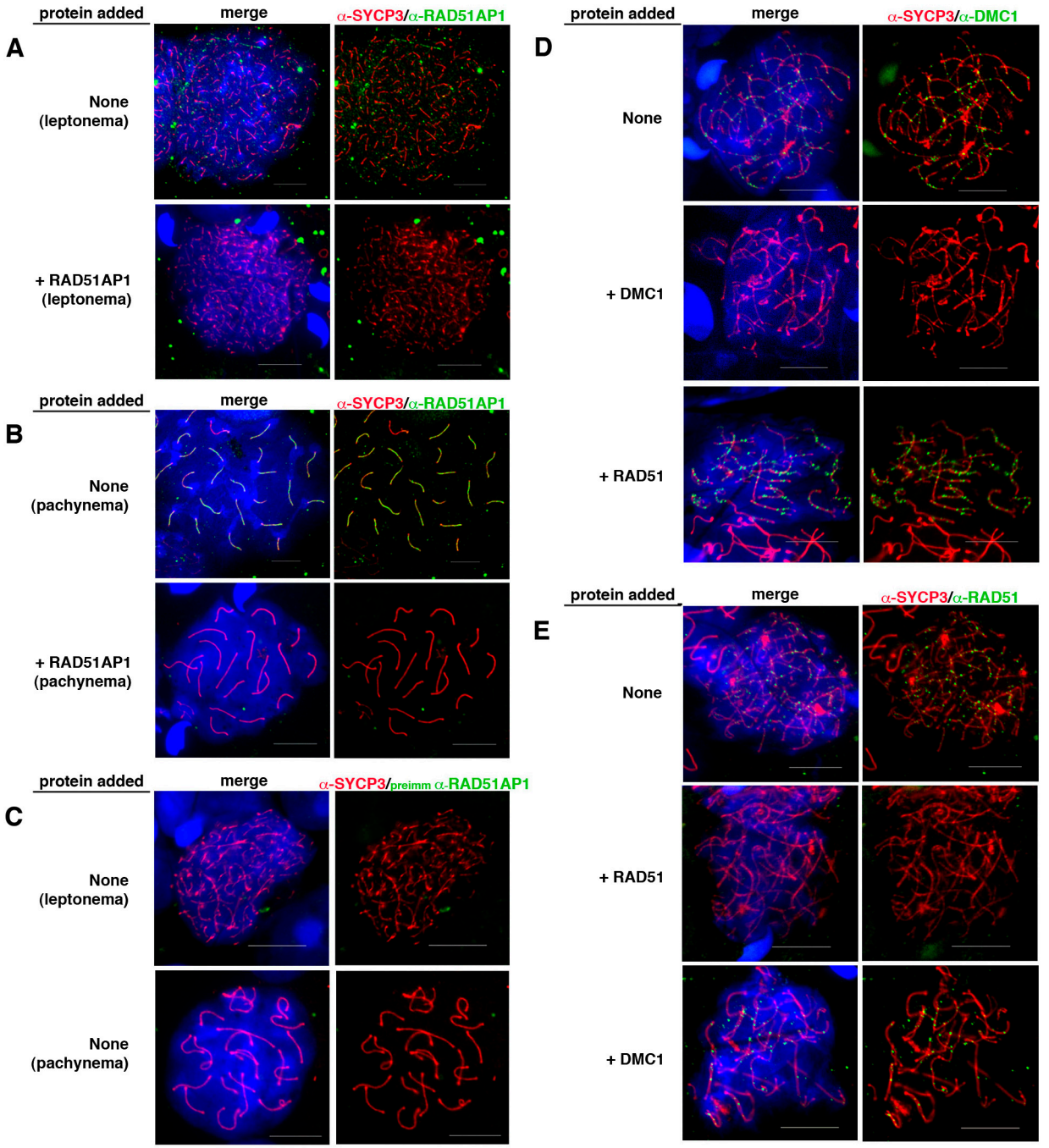

Fig. S7. *RAD51AP1, DMC1, and RAD51 antibody specificity.* (*A*) Example of a spermatocyte nucleus in leptonema. Chromosome spreads were stained with anti-SYCP3 (red) and anti-RAD51AP1 GP49 (green) antibodies. Class I and class II foci (as defined in Fig. S5) were no longer detected after incubation of the antibody preparation with RAD51AP1 protein. Class IV foci (speckles) remained. (*B*) Example of a spermatocyte nucleus in pachynema. Chromosome spreads were stained with anti-SYCP3 (red) and anti-RAD51AP1 GP49 (green) antibodies, then mounted with DAPI. Class III and class V foci (as defined in Fig. S5) were no longer detected after incubation of the antibody preparation with RAD51AP1 protein. Class IV foci remained. (*C*) Example of a spermatocyte nucleus in leptonema (*Top*) or pachynema (*Bottom*). Chromosome spreads were stained with anti-SYCP3 (red) antibody and preimmune GP49 serum (green). (*D*) Example of a spermatocyte nucleus in zygotene. Chromosome spreads were stained with anti-SYCP3 (red) and anti-DMC1 (green) antibodies. Axis-associated DMC1 foci were no longer detected after incubation of the antibody preparation with DMC1 protein, but incubation with RAD51 protein had little or no effect. (*E*) Example of a spermatocyte nucleus in zygotene. Chromosome spreads were stained with anti-SYCP3 (red) and anti-RAD51 (green) antibodies. Axis-associated RAD51 foci were no longer detected after incubation of the antibody preparation with RAD51 protein, but incubation with DMC1 protein had little or no effect. In *A*–*E* scale bar = 10 μm.

Table S1. Conservation of RAD51AP1 isoforms among vertebrates

Organism	Isoform 1	Isoform 2	Isoform 3
Human	352	335	302
Chimpanzee	352	335	302
Gorilla	352	—	—
Dog	354	—	—
Rock Hyrax	353	—	—
Bat	349	—	—
Horse	—	330	—
Cow	—	329	—
Chicken	—	346	—
Pig	—	340	—
Rat	—	337	—
Mouse	—	337	—
Tarsier	—	327	—
Frog	—	331	—

The various isoforms of RAD51AP1 were retrieved from www.ensembl.org and determined to be homologous to the human isoforms 1, 2, or 3 by sequence alignment. Numbers refer to total number of amino acid residues, i.e., 352 for 352 residues.

Table S2. Oligonucleotides used in this study

Name	Sequence	Nature	Assay
P1	5′-TTATATCCTTTACTTTGAATTCTATGTTTAACCTTTTACTTATTTTGTATTAGCCGG ATCCTTATTTCAATTATGTTCAT-3′	ssDNA	Duplex capture, EMSA
P2	5′-ATGAACATAATTGAAATAAGGATCCGGCTAATACAAAATAAGTAAAAGGTTAAA CATAGAATTCAAAGTAAAGGATATAA-3′	dsDNA	Duplex capture, EMSA
D1	5′-GCCGTGTCACTGGATCAGAGGTCACTTGGCAAGGATGGCCCGTCCGTAGCACCAG GACACCCTAGTTAGCTCCGACATGTCGTACATATCGGATGCTGGC-3′		
D2	5′-GCCAGCATCCGATATGTACGACATGTCGGAAATTAAGATGCAGCTTTGAAACTAA CCATTTCTACTGGATGCCAAGTGACCTCTGATCCAGTGACACGGC-3′		
D3	5′-TATGATTAGTCTAGGATTCTATTATCTATTAATGCTAGTCGCTAACTAGGGTGCCT GGTGCTACGGACGGGCCATCCTT-3′	D-loop substrate	EMSA
SspI	5′-AATGTTGAATACTCATACTCTTCCTTTTTCAATATTATTGAAGCATTTATC AGGGTTATT-3′	homologous	
AflIII	5′-CAGAATCAGGGGATAACGCAGGAAAGAACATGTGAGCAAAAGGCCAGC AAAAGCCAGGA-3′	heterologous	Synaptic assay
RT1	5′-ATGGTGCGTCCTACCAGAAATAGAAAACCA-3′		
RT2	5′-TACTTGGTTGGTGAGTGTTGGAAGTTCCTT-3′		
RT3	5′-GTTGCCCTGGCTTTATCTGTGAAGGAAC-3′		
RT4	5′-CCGCACTTGGCTGCTTGTGG-3′		RT-PCR